

## Nano Structure Iron (II) and Copper (II) Schiff Base Complexes of a NNO-Tridentate Ligand as New Antibiotic Agents: Spectral, Thermal Behaviors and DNA Binding Ability

Laila H. Abdel Rahman<sup>1,\*</sup>, Ahmed M. Abu-Dief<sup>1,\*</sup>, Samar Kamel Hamdan<sup>1</sup> and Amin Abdou Seleem<sup>2</sup>.

<sup>1</sup> Chemistry Department, Faculty of Science, Sohag University, 82534 Sohag, Egypt.

<sup>2</sup> Zoology Department, Faculty of Science, Sohag University, 82534 Sohag, Egypt.

Received: 28 Mar. 2015, Revised: 9 Apr. 2015, Accepted: 12 Apr. 2015.

Published online: 1 May 2015.

**Abstract:** Complexes of Fe (II) and Cu (II) with a tridentate Schiff base, 2-((z)-(pyridine-2-ylimino) methyl) naphthalene-1-ol derived from 2-hydroxy-1-naphthaldehyde and 2-aminopyridine were synthesized. Both the ligand and its complexes were characterized on the basis of microanalysis, melting point, <sup>1</sup>H and <sup>13</sup>CNMR, molar conductivity, thermal analysis, IR and UV/Vis spectral studies. From analytical data, the stoichiometry of the complexes was found to be 1: 2 (metal: ligand). The magnetic susceptibilities of all complexes at room temperature were consistent with octahedral geometry. The molar conductance values suggest nonelectrolytes. The IR spectra revealed that the metal ions coordinated through azomethine nitrogen, pyridine nitrogen of and phenolic oxygen of the ligand. The particle size of iron and copper complexes has been investigated by TEM. Antibacterial and antifungal activities in vitro were performed against *three* types of G+ and G- bacteria, *Escherichia coli*, *Pseudomonas aeruginosa*, *Staphylococcus aureus* and three types of fungi, *Aspergillus flavus*, *Trichophyton rubrum* and *Candida albicans* with determination of minimum inhibitory concentrations of ligand and metal complexes. Both complexes showed highly effective antibacterial activities against the tested bacteria and fungi; therefore, these complexes can be used as antibiotic. Furthermore, DNA interaction of Schiff base complexes was monitored by electronic spectra, hydrodynamic measurements and gel electrophoresis. It was found that the prepared complexes could bind to DNA in an intercalating mode.

**Keywords:** Synthesis, Characterization, Nano particles, Antimicrobial activity, Calf thymus DNA

## 1 Introduction

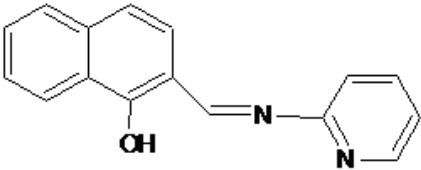
Schiff bases, which are potential chelating ligands in coordination chemistry [1], show promising applications in medicine as anti-oxidant, antimicrobial and anti-inflammatory [2, 3]. On the industrial scale, they have wide range of applications such as dyes and pigments precursors and corrosion inhibitors [4-6]. This can lead to many interesting catalytic and potential properties [7, 8]. In recent decades, metal complexes have received much attention in biochemistry and pharmacy as promising compounds for the creation of novel drugs [2, 9, 10].

These studies revealed that complexation of metal ions and different Schiff base ligands improves the bio potentials of the ligands. It is well accepted that metal ions can modify both magnitude and direction of the pharmacological activity of the initial organic compounds (ligands) as a result of changes in their size, shape, charge density distribution, and redox potentials [11]. Furthermore, the coordination compounds of biologically active Schiff base ligands have received much attention, and it has been

reported that chelation causes drastic change in the biological properties of the ligands and as well as the metal ions. Many drugs possess modified pharmacological and toxicological properties when administered in the form of transition metal complexes [12]. Compounds showing the properties of effective binding as well as cleaving double stranded DNA under physiological conditions; are of great importance since these could be used as diagnostic agents in medicinal and genomic research. Since the discovery of cisplatin [cis-diamminedichloroplatinum(II)], there has been a rapid expansion in research to find new and more efficacious metal-based anticancer drugs [13]. Amongst the non-platinum anticancer agents explored, considerable efforts have been put to design Ru (II)/(III) [14] organotin [15] and Cu(II) complexes [16]. Several recent review articles have summarized the advances in these fields [17, 18]. Further, copper accumulates in tumors because of the selective permeability of cancer cell membranes to copper compounds. For this reason a number of copper complexes were screened for anticancer activity and some of them were found active both in vivo and in vitro. Hence, it is very important to develop compounds with both strong

\* Corresponding author E-mail: Lailakenawy@hotmail.com, ahmed\_benzoic@yahoo.com

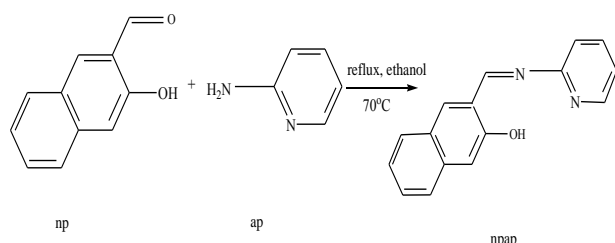
DNA-binding and antioxidant properties for effective cancer therapy. We report herein the results of our studies on the metal complexes of anile ligand (2-((Z)-(pyridin-2-ylimino) methyl) naphthalen-1-ol). Tentative structures have been proposed on the basis of analytical, spectral, magnetic, and conductance data. The prepared Schiff base and its metal chelates have been screened for biological activity against some strains of bacteria (G+ and G-) and fungi. In addition, the interaction behavior of these compounds with DNA has been explored by electronic spectra, hydrodynamic methods and gel electrophoresis.



(2-((Z)-(pyridin-2-ylimino)methyl)naphthalen-1-ol)  
(npap)

Metal	Acronym Ligand	Complex
Fe (II)	npap	npapFe
Cu (II)	npap	npapCu

**Scheme (1):** Structures and abbreviations of anil ligand and its corresponding complexes.



**Scheme (2):** Formation of the investigated Schiff base ligand where np = 2-hydroxy-1-naphthaldehyde and ap = 2-aminopyridine.

## 2 Experimental

### 2.1 Materials and methods

All chemicals and solvents used in this study such as 2-hydroxy-1-naphthaldehyde (np), 2-aminopyridine (ap) and the metal salts Cu (CH<sub>3</sub>COO)<sub>2</sub>.H<sub>2</sub>O and (NH<sub>4</sub>)<sub>2</sub>Fe(SO<sub>4</sub>)<sub>2</sub>.6H<sub>2</sub>O were of reagent grade and used as received. Calf thymus DNA (CT-DNA) and Tris [hydroxymethyl]-amino methane (Tris) were purchased from Sigma-Aldrich Chemie (Germany). Spectroscopic grade ethanol and HCl products were used.

Melting points were recorded on a Gallenkamp (UK)

apparatus. Perkin-Elmer model240c elemental analyzer was used to collect micro analytical data (C, H and N). <sup>1</sup>H and <sup>13</sup>CNMR of the ligands in deuterated dimethyl sulfoxide (DSMO) were recorded in BRUKER model 400 MHz. Molar Conductivities of the metal complexes determined in dimethyl sulphoxide (DSMO ~ 1×10<sup>-3</sup>M) at room temperature using Jenway conductivity meter model 4320. The magnetic susceptibilities of the complexes were determined on Gouy's balance and the diamagnetic correction were made by Pascal's constants and Hg[Co(SCN)<sub>4</sub>] as a calibrant [2].

The infrared spectra of the metal chelates were recorded on Shimadzu FTIR model 8101 in the region 400–4000 cm<sup>-1</sup> using KBr discs. UV-Vis spectral measurements for the synthesized complexes were made in DMF using 10mm matched quartz cells on PG spectrophotometer model T+80. Shimadzu cooperation 60H analyzer was used for thermogravimetric analysis (TGA) under a dynamic flow of nitrogen atmosphere (40 ml/min) and heating rate 10°C/min from ambient temperature to 750°C. HANNA 211 pH-meter was used for pH measurements at 298K and the pH values were adjusted using a series of Britton universal buffer [2, 19]. The particle size of the prepared complexes was analyzed using transmission electron microscope (TEM-2100), Faculty of Science, Alexandria University.

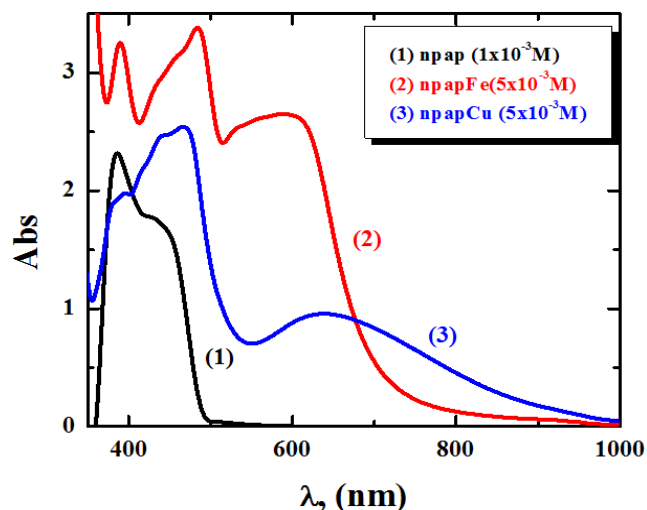


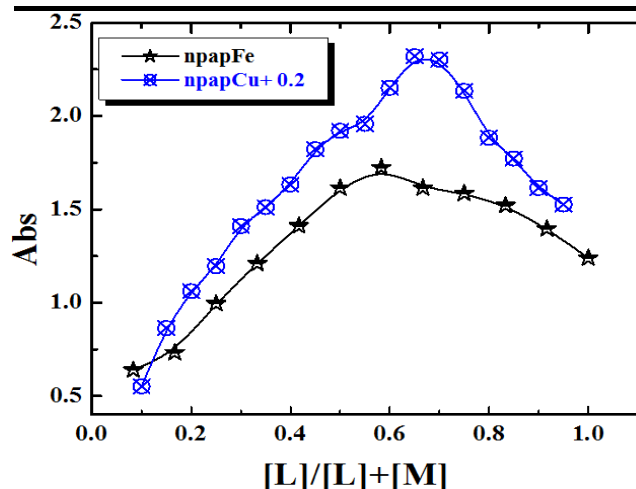
**Fig 1:** Molecular electronic spectra of (2) [npapFe] = 5×10<sup>-3</sup> M, (3) [npapCu] = 5×10<sup>-3</sup> M.

### 2.2 Synthesis of Schiff base ligand

An ethanolic solution of 5 mmole of 2-hydroxy-1-naphthaldehyde was mixed with a hot ethanolic solution of 5 mmole of 2-aminopyridine with constant stirring. The mixture was refluxed for approximately 1hr at 70°C and the solution was rotary evaporated to quarter of its original volume and then left to cool. After one day, the yellow crystals were isolated, washed with ethanol and then recrystallized in ethanol [2, 20].

**Table 1:** Analytical and physical data of the Schiff base ligand (npap) and its metal complexes.

Compound	M.wt	Color Yield (%)	$\Lambda_m$ $\Omega^{-1}\text{cm}^2$ mol $^{-1}$	$\mu_{\text{eff}}$	M.p Dec. (°C)	C found (calc.%)	H found (calc.%)	N found (calc.%)
npap	248.00	Yellow (78)	-	-	170	77.35 (77.42)	4.79 (4.84)	11.32 (11.29)
[Fe (npap) $_2$ ]. 2H $_2$ O	585.86	Brown (86)	4.70	4.95	> 300	65.42 (65.55)	4.39 (4.44)	9.49 (9.56)
[Cu (npap) $_2$ ].1.5H $_2$ O	584.55	Green (86)	6.02	2.18	> 300	65.58 (65.69)	4.09 (4.28)	9.43 (9.58)

**Fig. 2:** Continuous variation plots for the prepared complexes in aqueous -alcoholic medium at [npapFe] =  $5.00 \times 10^{-3}$  M, [npapCu] =  $1.00 \times 10^{-3}$  M and 298 K.

### 2.3 Synthesis of Schiff base complexes

The two complexes were synthesized by mixing the ethanolic solution of 5 mmole (20 ml) of the prepared Schiff base ligand with an equimolar amount of ethanolic solution of the metal salt. The resulting solutions were stirred magnetically for 3h [21, 22]. The obtained product was evaporated overnight. The formed solid product was filtered, washed with ethanol, and then dried in vacuo over anhydrous  $\text{CaCl}_2$ . In case of Fe (II) complex, few drops of glacial acetic acid [2, 3, 23] were added to avoid the oxidation of Fe (II) and the mixture solution was stirred magnetically for 3hr on cold under nitrogen at 25°C.

### 2.4 Evaluation of the stoichiometry of the Schiff base complexes:

The simplest spectrophotometric technique adopted to study the equilibria in solutions of complex compounds is the molar ratio method, [2, 24] and the continuous variation method [2, 25], as shown in Fig (2, 3).

### 2.5 Magnetic moment measurements:

Magnetic susceptibility measurements for the prepared

Schiff base complexes were calculated and listed in Table 1 according to the following relation [2, 26]:

$$\mu_{\text{eff}} = 2.83\sqrt{\chi'_M T}$$

$$\chi'_M = \chi_M - (\text{diamag. corr.})$$

Where T is the temperature (K),  $\mu_{\text{eff}}$  is the magnetic moment (in Bohr Magnetons) BM and  $\chi'_M$  is the molar magnetic susceptibility after correction.

### 2.6 Kinetic aspects

The thermodynamic activation parameters of the decomposition processes of the complexes were calculated using the Coats- Redfern equation [27],

$$\log \left[ \frac{\log(w_\infty / (w_\infty - w))}{T^2} \right] = \log \left[ \frac{AR}{\phi E^*} \left( 1 - \frac{2RT}{E^*} \right) \right] - \frac{E^*}{2.303RT}$$

Where W is the mass loss at the completion of the decomposition reaction. W is the mass loss up to temperature T, R is the gas constant and  $\phi$  is the heating rate. Since  $1 - 2RT/E^* \approx 1$ , the plot of the left-hand side of equation against  $1/T$  would give a straight line.  $E^*$  was then calculated from the slope and the Arrhenius constant, A, was obtained from the intercept. The other kinetic parameters; the entropy of activation ( $S^*$ ), enthalpy of activation ( $H^*$ ) and the free energy change of activation ( $G^*$ ) were calculated using the following equations:

$$S^* = 2.303R \log$$

$$H^* = E^* - RT$$

$$G^* = H^* - TS^*$$

Where (k) and (h) are Boltzmann's and Planck's constants, respectively. The Kinetic parameters are listed in Table 5.

### 2.7 Evaluation of the apparent formation constants of the synthesized complexes

The formation constants values ( $K_f$ ) of the studied Schiff base complexes were obtained from the

spectrophotometric measurements by applying the continuous variation method [6, 28] according to the following relation.

$$K_f = \frac{A/A_m}{4C^2 (1-A/A_m)^3}$$

The results are listed in Table 6. Where,  $A_m$  is the absorbance at the maximum formation of the complex,  $A$  is the arbitrary chosen absorbance values on either side of the absorbance mountain col (pass) and  $C$  is the initial concentration of the metal ions.

## 2.8. Pharmacological studies

### 2.8.1. Antibacterial screening

Antibacterial activity of Schiff base ligand and its metal complexes were tested against the bacterial species *Escherichia coli*, *pseudomonas aeruginosa* and *staphylococcus aureus* by following the standard disc diffusion method using nutrient agar medium [2, 23, 29]. Tetracycline was used as standards for antibacterial activity. The investigated ligand and its complexes were dissolved in dimethylsulfoxide (DMSO).

The Sterilized discs of agar plates and swabbed with the bacteria culture were filled with the test solution. The plates were incubated at 37° C for overnight. At the end of the incubation period, inhibition zones formed on the medium were evaluated in mm. DMSO was test as control under the same conditions for each organism and no activity was found. The activities of the prepared complexes were confirmed by calculating the activity index (cf. Table 9) according to the following relation [2, 30].

$$\text{Activity index (A)} = \frac{\text{inhibition zone of complex(mm)}}{\text{inhibition zone of standard drug(mm)}} \times 100$$

### 2.8.2. Antifungal screening

Standard potato dextrose agar was used as medium for antifungal activity by disc diffusion method [2, 31]. The antifungal activities of the compounds were evaluated by the disc diffusion method against the fungal microorganisms. The 5 mm diameter and 1 mm thickness of the disc was filled with the test solution using a micropipette and the plates were incubated at 37°C for 72 h. During this period, the test solution was diffused and affected the growth of the inoculated fungi. After 36 h of incubation at 37°C, the diameter of the inhibition was measured.

## 2.9 DNA binding studies

### 2.9.1 Electronic spectra

The DNA binding experiments of the metal complexes with CT-DNA were performed in Tris buffer (5 mM, pH 7.4). A solution of CT-DNA in the buffer gave a ratio of UV-Vis absorbance at 260 and 280 nm of about 1.9:1, indicating that the DNA was sufficiently free from protein [2, 23, 32, 33]. The DNA concentration per nucleotide and polynucleotide concentrations were determined by absorption spectroscopy using molar extinction coefficient ( $6600 \text{ M}^{-1}\text{cm}^{-1}$ ) at 260 nm [2, 23, 34, 35]. The intrinsic binding constant  $k_b$  for the interaction of metal (II) complexes with DNA has been calculated from the absorption spectral changes during the addition of increasing concentration of DNA according to the following equation:

$$\frac{[DNA]}{(\epsilon_a - \epsilon_f)} = \frac{[DNA]}{(\epsilon_b - \epsilon_f)} + \left[ \frac{1}{K_b (\epsilon_b - \epsilon_f)} \right]$$

Where,  $[DNA]$  is the concentration of DNA in base pairs, the apparent absorption coefficients  $\epsilon_a$ ,  $\epsilon_f$  and  $\epsilon_b$  correspond to  $A_{\text{obs}}/[\text{complex}]$ , extension coefficient for the complex in fully bound form respectively. The data were fitted to the above equation with slope equal to  $1/(\epsilon_b - \epsilon_f)$  and y-intercept equal to  $1/[k_b(\epsilon_b - \epsilon_f)]$  and the intrinsic binding constant  $k_b$  was obtained from the ratio of the slope to the intercept [36]. The standard Gibb's free energy for DNA binding was calculated from the following relation [2, 23, 37].

$$\Delta G_b^\circ = -RT \ln K_b$$

### 2.9.2 Viscosity study

Hydrodynamic volume change was measured using Ostwald viscometer immersed in a thermostatic bath maintained at  $37 \pm 0.1^\circ\text{C}$ . Flow times of each sample were measured with digital stopwatch. Mixing of the test compound and CT-DNA were done by bubbling nitrogen. Data are presented as  $(\eta/\eta_0)^{1/3}$  versus  $[\text{complex}] / [\text{DNA}]$ , where  $\eta$  is the viscosity of DNA in the presence of complex and  $\eta_0$  is the viscosity of DNA alone. Viscosity values were calculated from the observed flow time of DNA containing solutions ( $t$ ) corrected for that of buffer alone ( $t_0$ ),  $\eta = (t - t_0)$  [2, 23, 38].

### 2.9.3 Agarose gel electrophoresis

Agarose was purchased from Fischer-Biotech (GE Healthcare). Calf thymus DNA and a Ready-Load 100 bp DNA ladder were used as the native-size DNA and purchased from Bio labs. The samples were subjected to electrophoresis on 1% agarose gel prepared in TBE buffer (45 mM Tris, 45 mM boric acid and 1 mM EDTA, pH 7.3). Then 30  $\mu\text{l}$  from each of the incubated complex and DNA mixture was incubated for 30 min at 37 °C. Then it was loaded on the gel with tracking dye (0.25% bromophenol



blue, 40% sucrose, 0.25% xylene cyanole and 200 mM EDTA). The electrophoresis was performed at a constant voltage (100 V) for about 2 h (until bromophenol blue had passed through 50% of the gel) in TBE buffer. At the end of electrophoresis i.e. the end of DNA migration, the electric current was turned off. Then, the gel was stained by immersing it in water containing Ethidium bromide (0.5 µg/ml) for 30–45 min at room temperature and later visualized under UV light using a transilluminator and photographed with a Panasonic DMC-LZ5 Lumix Digital Camera [2, 39].

### 3 Results and discussion

The analytical data of ligand and metal complexes are given in Table 1. The elemental analyses show 1: 2 (metal: ligand) stoichiometry for the solid complexes, corresponding with  $[M(npap)_2]$ , where  $M = Fe(II)$  and  $Cu(II)$ . The magnetic susceptibilities of all complexes at room temperature were consistent with octahedral geometry.

#### 3.1 Molar conductivity

The molar conductivity ( $\Lambda_m$ ) data (4.70 – 6.04  $ohm^{-1}cm^2mol^{-1}$ ) measured at 25°C using  $10^{-3}$  M solutions of the complexes in DMF solvent. These low values indicate that all complexes are nonelectrolyte due to the absence of any counter ions in their structures [2, 23, 36, 37]. The molar conductance values of these complexes (Table 1) indicate that the Schiff base ligand (npap) is coordinated to the  $Fe(II)$  and  $Cu(II)$  ions as a mono negatively charged anions. Therefore, it seems that the two phenolic OH groups from the two ligand molecules have been deprotonated and bonded to the metal ions as oxygen anion [40].

#### 3.2 Infrared spectral studies

The IR spectra provide valuable information regarding the nature of function groups attached to the metal ion. The main infrared bands and their assignments are listed in Table 2. The spectrum of the Schiff base ligand exhibit characteristic band at 3426  $cm^{-1}$  due to the stretching

vibration of the OH group  $\nu(OH)$ . On other hand, the recorded IR spectra of the prepared complexes show broad band at 3434- 3455  $cm^{-1}$  which could be assigned to  $\nu(OH)$  stretching vibration of lattice water molecules [2, 23, 41, 42]. In IR spectra of metal complexes, the absence of a weak broad band at 3060-3300  $cm^{-1}$  indicates deprotonation of the intramolecular hydrogen-bonded OH on complexation.

The band appearing at 1630  $cm^{-1}$  due to azomethine of Schiff base ligand which was shifted to lower frequency by 16-20  $cm^{-1}$  in the complexes, indicating coordination of azomethine nitrogen to the metal ion [2, 23, 37, 43]. This was due to the donation of electron density from Nitrogen to metal. The IR spectrum showed a medium intensity band at 1538  $cm^{-1}$ , which is a characteristic of the coordinated pyridine nitrogen base [44]. The Schiff base ligand showed band at 1315  $cm^{-1}$  which can be assigned to stretching vibrations of the phenolic group (C-O). This band was shifted to lower wave number upon complexation denoting that the oxygen atom of the phenolic group is coordinated to the metal ion. IR spectra of metal complexes show bands at 478- 517  $cm^{-1}$  and 577-618  $cm^{-1}$  which can be assigned to (M-O) and (M-N), respectively [2, 23, 37, 45]. The other series of weak bands between 3000-3050  $cm^{-1}$  are related to CH aromatic stretching vibration [2, 23, 37, 46]. From the above facts, it is evident that coordination takes place via azomethine nitrogen, pyridine nitrogen and phenolic oxygen of the ligand.

#### 3.3 $^1H$ and $^{13}CNMR$ spectral for the prepared ligands

The proton NMR spectrum of the Schiff base ligand shows a singlet peak at 15.00 ppm [47] which corresponds to the phenolic group. The characteristic proton of azomethine appeared at 10.00 ppm [48]. The presence of signals at 8.50 and 8.20 ppm can be assigned to the protons of CH of pyridine. Signals of aromatic protons appeared in the range of 7.80-6.70 ppm. The  $^{13}CNMR$  spectra of the free ligand npap have showed a peak at 175.00 ppm due to characteristic azomethine carbon [49]. The signals at 152-108 ppm may be attributes to phenyl aromatic carbons.

**Table 2:** Infrared spectral data of the synthesized ligand and its complexes ( $cm^{-1}$ ).

Compound	$\nu(OH)/H_2O$	$\nu(CH)_{ar}$	$\nu(C=N)$	$\nu(C=N)_{py}$	$\nu(C-O)_{ph}$	$\nu(M-N)$	$\nu(M-O)$
npap	3426	3000(w)	1630 (s)	1585(sh)	1315(m)	-	-
npapFe	3434(b)	3050(w)	1610 (s)	1577(sh)	1250(m)	617(w)	517 (w)
npapCu	3455 (b)	3050(w)	1614 (s)	1563(sh)	1285(m)	577 (w)	478 (w)

**b = broad, s = sharp, sh = shoulder, w = weak, ar = aromatic, ph= phenolic**

**Table 3:** Characteristic UV-Vis bands (nm) for imine ligand (npap) and its metal complexes.

Compound	$\lambda_{\max}(\text{nm})$	$\epsilon_{\max}$ ( $\text{dm}^3 \text{mol}^{-1} \text{cm}^{-1}$ )	Assignment
npap	325	3074	$\pi \rightarrow \pi^*$
	395	2392	$n \rightarrow \pi^*$
	423	1823	$n \rightarrow \pi^*$
npapFe	397	660	Intraligand band
	486	683	LCMT band
	582(b)	536	d-d band
npapCu	397	405	Intraligand band
	466	515	LCMT band
	637(b)	196	d-d band

b = broad

**Table 4:** TGA results of the prepared metal complexes in nitrogen atmosphere.

Compound	Dec. Temp(°C)	Weight loss (%) Found (Calcd)	Dec. assignment	Residue (%) Found (Calcd)
npapFe	15-135 °C	6.17 ( 6.14)	2H <sub>2</sub> O	
	135-394 °C	33.40 (33.29)	C <sub>12</sub> H <sub>7</sub> N <sub>2</sub> O	Fe 9.37 (9.53)
	394-581 °C	51.06 (51.02)	C <sub>20</sub> H <sub>15</sub> N <sub>2</sub> O	
npapCu	31-116 °C	4.61 ( 4.64)	1.5H <sub>2</sub> O	
	118-274 °C	18.21 (17.93)	C <sub>6</sub> H <sub>5</sub> N <sub>2</sub>	Cu 10.54 (11.03)
	275-528 °C	66.62 (66.43)	C <sub>26</sub> H <sub>17</sub> N <sub>2</sub> O <sub>2</sub>	

### 3.4 Electronic spectra

The electronic spectra of the Schiff base ligand and its complexes are summarized in Table 3. The spectrum of the free ligand exhibit bands at about 325, 395 and 423nm. The first peak is attributed to  $\pi \rightarrow \pi^*$  transitions. This band was not significantly affected by chelation. The second and third peaks in the spectrum of ligand are assigned to  $n \rightarrow \pi^*$ .

These bands disappeared via complexation and new band attributed to the donation of the lone pair of electrons of the nitrogen atoms of the Schiff base to metal ion ( $M \rightarrow N$ ) appear [50]. Comparing these with  $n \rightarrow \pi^*$  transition, these bands were shifted to longer wavelength along with increasing in its intensity. All complexes show a band in the range 582- 637 nm, which is attributed to  $d \rightarrow \pi^*$  transition that is mixed with  $d \rightarrow d$  transition. The study of the electronic spectra to identify the  $d \rightarrow d$  transitions in the presence of ligand field has encountered because several bands fall in the near-infrared region with a low intensity while a large part of the visible region is obscured by intense charge transfer and intraligand ( $\pi \rightarrow \pi^*$ ) transitions [2,23, 37, 51]. These electronic transitions along with magnetic moment 4.95 B.M. and 2.18 B. M. suggest octahedral geometry for Fe (II) and Cu (II) complexes.

### 3.5 Thermogravimetric analysis

Thermal studies of metal complexes were carried out using thermogravimetric technique (TG) and differential thermogravimetric (DTG). Table 4 gives the detailed thermal decomposition data for the studied complexes. The thermal decomposition results of Cu (II) complex takes place in three stages. The first stage of decomposition is noticed in the temperature range 32 -116 °C. It is due to the elimination of hydrated water molecule. The mass loss observed in this step is 4.61 % against the calculated loss of 4.64%. The second stage of decomposition occurs in the temperature range of 118–274°C, due to melting and partial decomposition of the ligand. This step bringing the weight loss of 18.21 % (calc. 17.93 %). The decomposition range (275–528 °C) of weight loss in third stage gives 66.62 % (calc. 66.43 %). This is due to the decomposition of the ligand molecule. The complex is present in the form of its metal above 500 °C.

### 3.6 Kinetic parameters of metal complexes

The kinetic parameters *Viz*, the energy of activation ( $E^*$ ), the entropy of activation ( $\Delta S^*$ ) and the Gibbs energy change ( $\Delta G^*$ ) were determined by the Coats–Redfern integral method. The obtained data are given in Table 5.

Form the obtained results; it is apparent that  $G^*$  values of the complexes acquire highly positive magnitudes. The activation energies of decomposition were found to be in the range 12.51- 57.32 KJ mol<sup>-1</sup>. The high value of the energy of activation of the complexes due to their covalent character. The negative values of  $S^*$  for the degradation process indicated more ordered activated complex than the reactants and assigned to slow decomposition reaction.

### 3.7 Magnetic moment measurements

Magnetic moment of the complexes was observed at room temperature. The iron complex shows  $\mu_{\text{eff}}$  value in the region 4.95 B.M. due to presence of four unpaired electrons. The room temperature value of Copper ion for complex is 2.18 B.M, which is consistent with one unpaired electron ( $d^9$ ). It is possible that the Copper (II) complexes have octahedral geometry. The observed magnetic moment of 4.95 B.M and 2.18 B.M along with electronic transitions corresponds to octahedral geometry for the two complexes.

### 3.8 Evaluation of the stoichmetry of the Schiff base ligands complexes:

The curves of continuous variation methods displayed maximum absorbance at mole fraction X ligand = 0.65 in Fe(II) and Cu(II) complexes, indicating the formation of complexes with metal ion to ligand ratio 1:2 as presented in schemes 3. Moreover, the data resulted from applying the molar ratio method support the same metal ion to ligand ratio of the prepared complexes cf. Fig 2, 3.

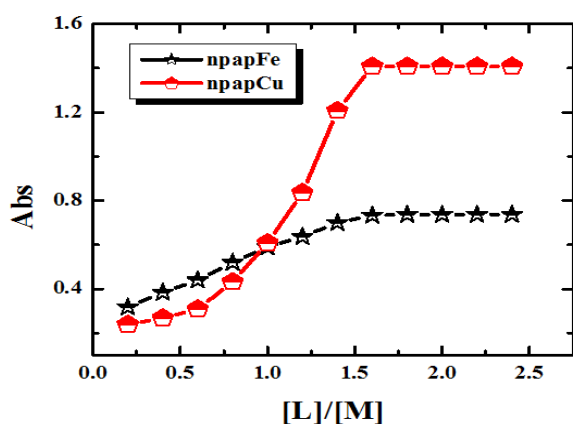
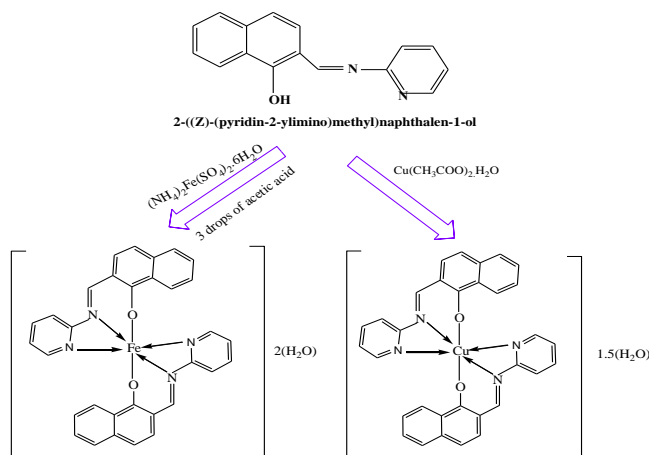


**Fig.3:** Molar ratio plots for the studied complexes in aqueous-alcoholic mixture at  $[M] = [\text{Fe}] = 5.00 \times 10^{-3} \text{ M}$ ,  $[\text{npap}] = 5.00 \times 10^{-3} \text{ M}$  and  $[M] = [\text{Cu}] = 1.00 \times 10^{-3} \text{ M}$ ,  $[\text{npap}] = 1.00 \times 10^{-3} \text{ M}$ .



**Scheme (3):** Formation of the investigated iron (II) and copper (II) complexes.

### 3.9 Evaluation of the apparent formation constants of the synthesized complexes

As mentioned in Table 6, the obtained ( $K_f$ ) values indicate the high stability of the prepared complexes. The values of ( $K_f$ ) for the studied complexes increase in the following order:  $\text{npapCu} > \text{npapFe}$ . Moreover, the values of the stability constant ( $\text{pK}$ ) and Gibbs free energy of investigated complexes are cited in the same Table 6. The negative values of Gibbs free energy mean that the reaction is spontaneous and favorable.

The pH-profile (absorbance vs. pH) presented in Fig.4 showed typical dissociation curves and a wide stability pH range (5-10) of the studied complexes. This means that the formation of the complex greatly stabilizes the Schiff base ligands [2, 23, 37].

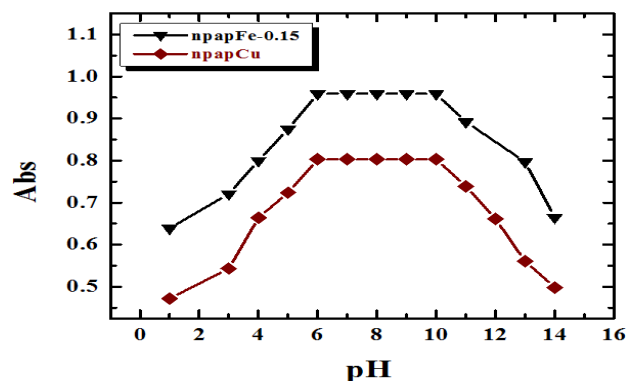


**Fig.4:** pH-profile of the prepared complexes at  $[\text{complex}] = 1.00 \times 10^{-3} \text{ M}$ .

**Table 5:** Kinetic parameters of the prepared metal complexes.

Complex	T (°C)	H* (KJ.mol <sup>-1</sup> )	S* (KJmol <sup>-1</sup> K <sup>-1</sup> )	G* (KJ.mol <sup>-1</sup> )
npapFe	27-207°C	-0.81	-0.158	16.44
	207-308°C	-2.06	-0.165	40.91
	308-392°C	-2.75	-0.167	54.72
npapCu	16-106 °C	-0.59	-0.151	12.51
	106-369 °C	-1.92	-0.166	39.22
	369-531 °C	-2.91	-0.167	57.32

### 3.10. Morphological structures of the prepared complexes

From TEM images and the calculated histogram (cf. Fig. 5 (a-d)), it is observed that the prepared complexes have particle size of 80 nm and 40 nm for iron (II) and copper (II) complexes respectively. This results indicate that the prepared complexes have a high surface area and this can lead to many interesting catalytic and potential properties [52].

### 3.11 Biological evaluation of synthesized complexes

**Table 6:** The formation constant ( $K_f$ ), stability constants (pK) and Gibbs free energy values of the synthesized complexes in DMF at 298K.

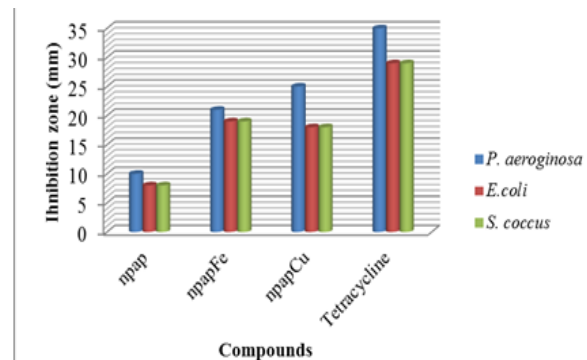
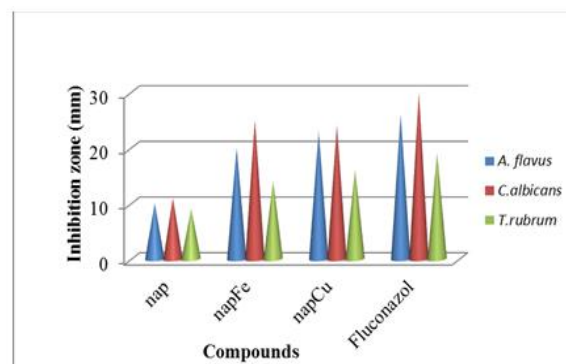
Complex	Type of complex	$K_f$	pK	G (KJ mol <sup>-1</sup> )
npapFe	1:2	$17.92 \times 10^9$	23.61	-58.49
npapCu	1:2	$13.39 \times 10^{11}$	27.92	-69.18

**Table 7:** Bactericidal activity of Schiff base ligand and its metal complexes.

Compound	Inhibition zone (mm)					
	<i>Pseudomonas aeruginosa</i> (-ve)		<i>Escherichia coli</i> (-ve)		<i>Staphylococcus aureus</i> (+ve)	
	10	25	10	25	10	25
npap	5	10	4	8	7	12
npapFe	10	21	8	19	16	29
npapCu	11	25	9	18	16	31
Tetracycline	21	35	16	29	24	39

Chelation reduces the polarity of the metal ion considerably, mainly because of the partial sharing of its positive charge with donor groups and possible  $\pi$  electron delocalization on the whole chelate ring [54].

The lipid and polysaccharides are some important constituents of cell walls and membranes, which are preferred for metal ion interaction. In addition to this, the cell wall also contains many aminophosphates, carbonyl and cysteinyl ligands, which maintain the integrity of the

**Fig 6:** Histogram showing the comparative activities of the compounds against different strains of bacteria (*p. aeruginosa*, *E. coli* and *S. aureus*) at 25mg /ml.**Fig.7:** Histogram showing the comparative activities of the compounds against different strains of fungi (*A. flavus*, *C. albicans* and *T. rubrum*) at 25 mg /ml.

membrane by acting as a diffusion barrier and also provides suitable sites for binding. Chelation can reduce not only the polarity of the metal ion, but it increases the lipophilic character of the chelate, and the interaction between metal ion and the lipid is favoured [55].

This may lead to the breakdown of the permeability barrier of the cell, resulting in interference with the normal cell processes. Accordingly, the antimicrobial activity of the two complexes can be referred to the increase of their lipophilic character which in turn deactivates enzymes responsible for respiration processes and probably other cellular enzymes, which play a vital role in various



metabolic pathways of the tested microorganisms. The toxicity of the metal complexes can be related to the strength of the metal- ligand bond, besides other factors such as size of the cation, receptor sites, diffusion and a combined effect of the metal and the ligands for inactivation of the biomolecules.

**Table 8:** Fungicidal screening of Schiff base ligand and its metal complexes.

Compound	Inhibition zone (mm)					
	<i>Aspergillus Flavus</i>		<i>Candida albicans</i>		<i>Trichophyton rubrum</i>	
	10	25	10	25	10	25
npap	6	10	7	11	4	9
npapFe	10	20	16	25	9	14
npapCu	13	23	17	24	11	16
Fluconazole	14	26	19	30	12	19

### 3.11.1 In vitro antimicrobial activity

The ligand and the metal complexes have been screened for their antibacterial and antifungal activity. The results obtained are presented in Tables (7, 8).

It is observed that all the metal complexes exhibited a more inhibitory effect compared to the ligand. This is probably due to greater lipophilic nature of the complexes. It was evident from the data that this activity increased on coordination. This enhancement in the activity can be explained on the basis of chelation theory [53].

## 3.12 DNA binding affinity of metal (II) complexes

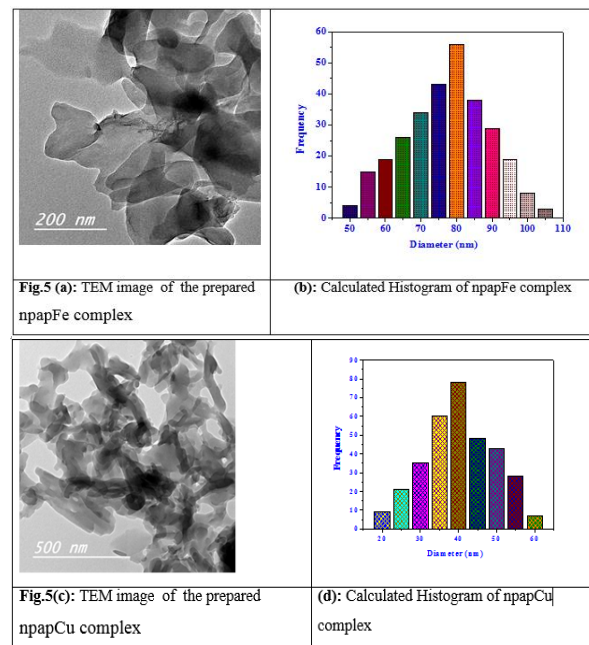
### 3.12.1 Electronic spectral studies

The absorption spectral titration method is one of the most important techniques which have usually been utilized to monitor the interaction of metal complex with and DNA. The binding of an intercalative complex molecule to DNA has been well characterized by notable intensity decrease (hypochromism) and red shift (bathochromism) of the electronic spectral bands due to strong stacking interaction between the aromatic chromophore of the ligand and DNA base pairs. The degree of hypochromism and the size of the red shift depend on strength of the intercalative interaction [56-58]. On the other hand; metal complexes which do not intercalate or interact electrostatically with DNA may exhibit hyperchromism [59]. The electronic spectra of Cu (II) complex in the absence and presence of CT-DNA are given in Fig. 8.

The absorption spectra show clearly that the addition of DNA to iron and copper complexes yields a significant hypochromism and a slight red shift at MLCT band. The  $K_b$  values of Fe(II) and Cu(II) complexes were determined to be  $1.36 \times 10^5$ ,  $1.05 \times 10^5$   $M^{-1}$ , respectively, indicating that the order of binding affinity between compounds Fe(II) complex > Cu(II) complex. However, the determined  $K_b$  values are lower than those observed for typical classical intercalators (ethidium bromide EB,  $K_b = 1.46 \times 10^6$ ) [60].

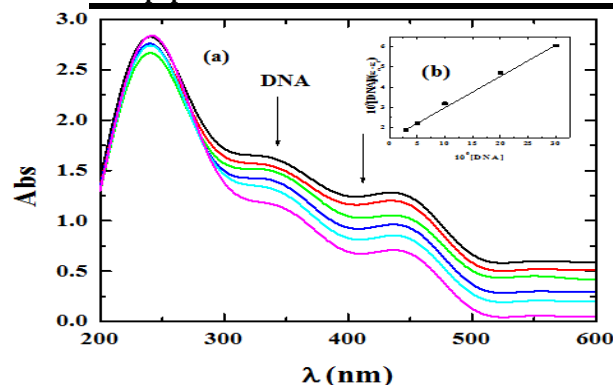
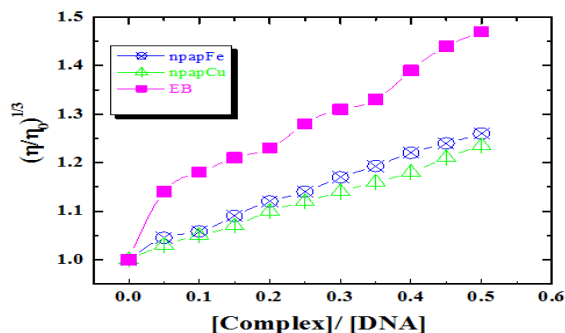
### 3.12.2 Hydrodynamic studies

In order to clarify the interactions between the compounds and DNA, viscosity measurements were carried out. Hydrodynamic measurements that are sensitive to length change (i.e. viscosity and sedimentation) are regarded as the least ambiguous and the most critical tests of binding in solution in the absence and presence of crystallographic structural data [61]. The effects of all the synthesized complexes on the viscosity of DNA at  $30 \pm 0.1^\circ C$  are shown in Fig .9. Viscosity experimental results clearly show that all the complexes can intercalate between the adjacent DNA base pairs, causing an extension in the helix, and thus increase the viscosity of DNA [62, 63]. The complexes can intercalate strongly, leading to a greater increase in the viscosity of DNA with an increasing concentration of complexes. The increased degree of viscosity which follow the order of npapFe > npapCu may depend on its affinity to DNA.

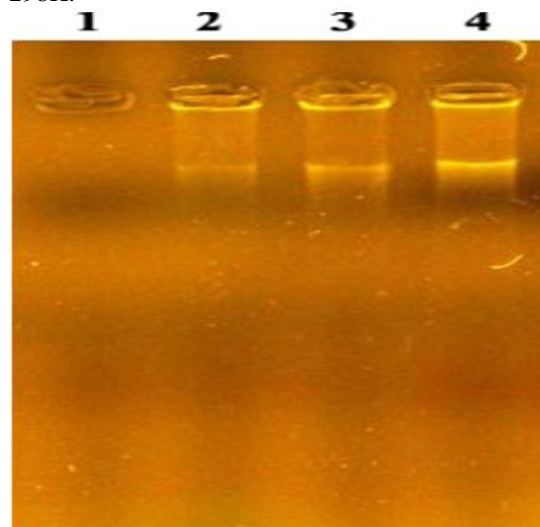


**Table 9:** Results of activity index (%) of the prepared Schiff base ligand and its complexes against different strains of bacteria and fungi.

Compound	Bacteria				Fungi	
	<i>P. aeruginosa</i>	<i>E. coli</i>	<i>S. coccus</i>	<i>A. flavus</i>	<i>C. albicans</i>	<i>T. rubrum</i>
npap	38.57	27.59	30.77	28.57	36.67	47.37
npapFe	60.00	65.52	74.36	76.92	83.33	73.68
npapCu	71.14	62.07	79.49	88.46	80.00	84.21

**Fig 8:** (a) Absorption titration of npapCu complex ( $1 \times 10^{-3}$  M) in the absence and presence of increasing amounts of CT-DNA (3-30)  $\mu$ M at room temperature in 0.01 M Tris buffer (pH 7.4 at 25°C) (b) Plot of [CTDNA]/( $\epsilon_a - \epsilon_f$ ) vs. [CT-DNA] for the titration of CT-DNA with npapCu complex.**Fig 9:** The effect of increasing the amount of the synthesized complexes on the relative viscosities of DNA

at [DNA] = 0.5 mM, [complex] and [EB] = 25–250  $\mu$ M and 298K.

**Fig 10:** The interaction of the investigated complexes with DNA was studied by gel electrophoresis, where Lane 1: blank, Lane 2: CT-DNA+ npapFe, Lane 3: CT-DNA+ npapCu, Lane 4: CT-DNA alone.

### 3.12.3 Gel electrophoresis

The DNA cleavage of metal complexes was studied by electrophoresis and the results were represented in Fig 10. The intensity of lanes was increased in the sequence npapFe > npapCu and these are in a good agreement with binding constant values of the investigated complexes with CT-DNA (cf. Table10).

**Table 10:** Optical properties of metal complexes with addition of DNA and their binding constants,  $K_b$ .

Complex	$\lambda_{\text{max}}$ free	$\lambda_{\text{max}}$ bound	$\Delta n$ (nm)	Binding constant ( $10^5 K_b$ ) <sup>a</sup>	Chromism (%) <sup>b</sup>	Type of chromism	$\Delta G^*$ (KJ.mol <sup>-1</sup> )
npapFe	223.00	230.22	1.01	1.36	30.69	Hypo	-29.29
	439.25	440.30	1.06		96.77		
npapCu	315.00	315.00	0	1.05	10.36	Hypo	-28.64
	443.83	445.13	2.30		36.01		

**a** intrinsic dna binding constant form the uv-vis absorptionspectral titration.

**b** chromism (%)=[Abs free - Abs bound/abs free) x100]

## Conclusion

The present paper reports the synthesis and spectroscopic characterization of a novel tridentate Schiff base ligand and its metal complexes. On the basis of physicochemical and spectral data discussed above, octahedral geometry for Fe (II) and Cu (III) complexes is proposed. IR spectra show the ligand as ONN tridentate, coordinating via azomethine-nitrogen, phenolic-oxygen and pyridine nitrogen. Thermal study reveals that the complexes are thermally stable. The conductance measurements show that all the metal complexes are non-electrolytes in nature. The DNA binding study takes place via an intercalative mode. These findings clearly indicate that transition metal based complexes have many potential practical applications, like the development of nucleic acid molecular probes and new therapeutic reagents for diseases. The results of antimicrobial activity show that the metal complexes exhibit antimicrobial properties and it is important to note that they show enhanced inhibitory activity compared to the parent ligand under identical experimental conditions. The antibacterial activity has been explained on the basis of chelation theory.

## Acknowledgments

The authors thank Dr. Ayman Nafady Associate Professor of Electrochemistry and Renewable Energy, Chemistry Department, Faculty of Science, Sohag University, Egypt and Department of Chemistry College of Science, King Saud University Riyadh, Saudi Arabia for his significant revision and language editing of the manuscript.

## References

- [1] Y. Inada, K. Mochizuki, T. Tsuchiya, H. Tsuji, S. Funahashi, *Inorganica Chimica Acta*, **358**: 3009–3014, (2005).
- [2] L.H. Abdel-Rahman, R.M. El-Khatib, L. A.E. Nassr, Ahmed M. Abu-Dief, M. Ismail, A.A. Seleem, *Spectrochimica Acta Part A: Molecular and Biomolecular Spectroscopy*, **117**, 366, (2014).
- [3] L. H. Abdel-Rahman, R. M. El-Khatib, L. A. E Nassr, A. M. Abu-Dief, *International Journal of Chemical Kinetics* **46**, 543-553, (2014).
- [4] H.M. Abd El-Lateef, A.M. Abu-Dief, L.H. Abdel-Rahman, E.C. Sañudo, N. A. Alcalde, *Journal of Electroanalytical Chemistry*, **743**, 120–133, (2015).
- [5] C.T.K. Kumar, J. Keshavayya, T. Rajesh, S.K. Peethambar, *International Journal of Pharmacy & Pharmaceutical Science*, **5**, 1, (2003).
- [6] A. M. Abu-Dief, R. Díaz-Torres, E. C. Sañudo, L. H. Abdel-Rahman, N. Aliaga-Alcalde, *Polyhedron*, **64**, 203, (2013).
- [7] A. El-Motaleb M. Ramadan, M. M. Ibrahim, S. Y. Shaban, *Journal of Molecular structure* **1006**, 348–355(2011).
- [8] P. Viswanathamurthi, K. Natarajan, *Synthesis and Reactivity in Inorganic and Metal-Organic Chemistry*, **36**, 415–418, (2006).
- [9] L.H. Abdel-Rahman, R.M. El-Khatib, L. A.E. Nassr, A. M. Abu-Dief, *International Journal of Nanomaterials and Chemistry*, **1**, 25-30, (2015).
- [10] L.H. Abdel-Rahman, R.M. El-Khatib, L. A.E. Nassr, A. M. Abu-Dief, *Russian Journal of General Chemistry*, **84**, 9, 1830–1836, (2014).
- [11] R.N Patel, *Inorganica Chimica Acta*, **363**: 3838–3846, (2010).
- [12] W. U. Huilu, F. Kou, F. Jia, B. Liu, J. Yuan, Y. Bai, *Journal of Photochemistry and Photobiology B: Biology*, **105**: 190–197, (2011).
- [13] I. Kostova, *Recent Patents Anticancer Drug Discovery*, **1**, 1- 22, (2006).
- [14] M. Glanski, V.B. Arion, M.A. Jakupc, B.K. Keppler, *Current Pharmaceutical Design*, **9**, 2078-2089, (2003).
- [15] A. Alama, B. Tasso, F. Novelli, F. Sparatore, *Drug Discovery Today* **14**, 500-508, (2009).
- [16] C. Marazano, M. Pellei, F. Tisato, C. Santini, *Anti-cancer Agents in Medicinal Chemistry*, **9**, 185-211, (2009).
- [17] L. Ronconi, P.J. Sadler, *Coordination Chemistry Reviews*, **251** 1633-1648, (2007).
- [18] R. Nagane, M. Chikira, M. Oumi, H. Shindo, W.E. Antholine, *Journal of Inorganic Biochemistry*, **78**, 243-249, (2000).
- [19] H.T.S. Britton, *Hydrogen Ions*, fourth ed., Chapman and Hall, London, UK, (1952).
- [20] A. P. Mishra, R.K. Jain, *Journal of Chemical and Pharmaceutical Research*, **2**, 6, 51-61, (2010).
- [21] E.V. Sekhar, K.N. Jayaveera, S. Srihari, *Journal of Chemical and Pharmaceutical Research*, **4**, 12, 5121-5125, (2012).
- [22] M.A. Neelakantan, M. Esakkiimmal, S.S. Mariappan, J. Dharmaraja, T. Jeyakumar, *Indian Journal of pharmaceutical Science*, **72**(2), 216-222, (2010).
- [23] L.H. Abdel-Rahman, R. M. El-Khatib, L.A.E. Nassr, A. M. Abu-Dief, F. El-Din Lashin, *Spectrochimica Acta Part A: Molecular Biomolecular Spectroscopy*, **111**, 266–276, (2013).
- [24] R. El-Shiekh, M. Akl, A. Gouda, W. Ali, *Journal of American Science*, **7** (4) 797–807(2011).

- [25] P. Job, *European Journal of Organic Chemistry*, **9** 113–203(1928).
- [26] L. H. Abdel-Rahman, R. M. El-Khatib, L. A.E. Nassr, Ahmed M. Abu-Dief, *Arabian Journal of Chemistry*, in press (2013).
- [27] A.W. Coats, *Journal of Polymer Science Part B: Polymer Letters*, **3**, 11, 917-920, (1965).
- [28] N. Raman, J.D. Raja, A. Sakthivel, *Journal of Chemical Science*, **119** (4), 303–309, (2007).
- [29] M.J. Pelczar, E.C.S. Chan, N.R. Krieg, Microbiology, Fifth ed., Tata McGraw Hill Publishing Co., Ltd, New Delhi, (1998).
- [30] N. Raman, J. D. Raja, A. Sakthivel, *Journal of Chemical Science* **119** (4), 303–309 (2007).
- [31] J. Marmur, *Journal of Molecular Biology*, **3**, 208–218, (1961).
- [32] M. Sirajuddin, S. Ali, A. Haider, N.A. Shah, A. Shah, M.R. Khan, *polyhedron* **40**, 19-31, (2012).
- [33] M. Tarqi, N. Muhammad, M. Sirajuddin, S. Ali, N.khalid, M.R. Khan, M.N. Tahir, *Journal of Organometallic Chemistry* **723**, 79- 89(2013).
- [34] M. Tarqi, S. Ali, N. Muhammad, N.A. Shah, M. Sirajuddin, M.N. Tahir, N. Khalid, M.R. Khan, *Journal of Coordination Chemistry* **67**, 323-340, (2014).
- [35] M. Sirajuddin, S. Ali, F.A. Shah, M. Ahmed, M.N. Tahir, *Journal of the Iranian Chemical Society*, **11**, 297-313, (2014).
- [36] A. Wolfe, G. H. Shimer, T. Meehan, *Journal of Biochemistry*, **26**, 6392–6396 (1987).
- [37] L.H. Abdel-Rahman, R. M. El-Khatib, L. A.E. Nassr, A. M. Abu Dief, *Journal of Molecular Structure*, **1040**, 9-18, (2013).
- [38] S. Basili, A. Bergen, F. D. Acqua, A.Ranzhan, H. Ihmels, S. Moro, G. viola, *Journal of Biochemistry* **46** (44) ,12721-12736, (2007).
- [39] D. Sabolová, M. Koz ůrková, T. Plichta, Z. Ondrušová, D. Hudecová, M. Simkovic, H. Paulíková, A. Valent, *International Journal of Biological Macromolecules*, **48**, 319–325, (2011).
- [40] B. Geeta, K. Shravankumar, P. R. Muralidhar, E. Ravikrishna, M. Sarangapani, K. R. Krishna, and V. Ravindera: *Spectrochimica Acta Part A*, **77**, 911–915(2010).
- [41] A. A. Emara, *Spectrochimica Acta Part A: Molecular and Biomolecular Spectroscopy*, **77**, 117–125 (2010).
- [42] E.M. Hossain, N.M. Alam, J. Begum, A.M. Akbar, M. Nagimuddin, E.F. Smith, C.R. Hynes, *Inorganica Chimica Acta*, **249**, 207-213(1996).
- [43] A.M. Shaker, A.M. Awad, L.A.E. Nassr, Synthesis and Reactivity in Inorganic and Metal-Organic Chemistry **33**, (1), 103–107, (2003).
- [44] N. Nishat, R.U. Din, M.M. Haq, *Transition Metal Chemistry*, **28**, 948 (2003).
- [45] K. Nakamoto, Infrared Spectra of Inorganic and Coordination Compounds, *Wiley Inter Science*, **435**, (1970).
- [46] M.B. Ferrari, F. Bisceglie, G. Pelosi, P. Tarasconi, *Polyhedron* **27**, 1361–1367, (2008).
- [47] A.M.A. Alaghaz, B. A. El-Sayed, A.A. El-Henawy, R. A.A. Ammar, *Journal of Molecular Structure*, **1035**, 83-93, 2013.
- [48] G. Gehad, Z. Abd El-wahab, *Spectrochimica Acta Part A: Molecular and Biomolecular Spectroscopy*, **61**, 1059- 1068, (2005).
- [49] M. Gullotti, A. Pasini, P. Fantucci, R. Ugo, R.D. Gillard, *Gazz. Chim. Ital.* **102**, 855, (1972).
- [50] K. G. Sushil, Chanda, S. Neha, J. B. Ray, P. J. Jerry, A. G. James, *Polyhedron*, **89**, 219–231, (2015).
- [51] B.N. Ghose, K.M. Lasisi, Synthesis and Reactivity in Inorganic, *Metallic-Organic Chemistry*, **16**, 1121-1133(1986).
- [52] M. A. A. Ali El-Remaily, A. M. Abu-Dief, *Tetrahedron*, **71**, 2579-2584, (2015)
- [53] A.B.P. Lever, *Journal of Molecular Structure*, **129**, 180-181, (1985).
- [54] Z. H. A. Wahab, M. M. Mashaly, A. A. Salman, B. A. El-Shetary, A. A. Faheim, *Spectrochimica Acta Part A: Molecular and Biomolecular Spectroscopy*, **60**, 2861- 2873, (2004).
- [55] Z.H. Chohan, K.M. Khan, C.T. Supuran, *Journal of Applied Organometallic Chemistry*, **18**, 305, (2004).
- [56] J.M. Kelly, A.B. Tossi, D.J. McConnell, C. Ohuigin, *Nucleic Acids Reviews*, **13**, 6017- 6034, (1985).
- [57] A. Sitlani, E.C. Long, A.M. Pyle, J.K. Barton, *Journal of American Chemical Society*, **114**, 2303-2312, (1992).
- [58] S.A. Tysoe, R.J. Morgan, A.D. Baker, T.C. Streckas, *Journal of Physical Chemistry*, **97**, 1707-1711, (1993).
- [59] D. Mandal, M. Chauhan, F. Arjmand, G. Aromi, D. Ray, *Journal of the Chemical Society, Dalton Transactions*. 9183-493, (2009).

- [60] R. Indumathy, M. Kanthimathi, T. Weyhermuller, B.U. Nair, *Polyhedron*, **27**, 3443-3450, (2008).
  - [61] A. Hartwig, *Chemico-Biological Interactions*, **184**, 269–272, (2010).
  - [62] J.N. Wheate, R.C. Brodie, G.J. Collins JG, R.J. Kemps, R.J. Aldrich-Wright, *Mini-Reviews In Medicinal Chemistry*, **627**-684,(2007).
  - [63] P.R. Hertzberg, P. B. Dervan, *Journal American of Chemical Society*, **104**, 313-315, (1982).
-